



Do not break a sweat: avoiding pitfalls in the diagnosis of sweat gland tumors

Thomas Brenn ^{1,2}

Received: 24 June 2019 / Revised: 10 September 2019 / Accepted: 11 September 2019 / Published online: 26 September 2019
© The Author(s), under exclusive licence to United States & Canadian Academy of Pathology 2019

Abstract

The group of malignant sweat gland neoplasms is characterized by a wide biologic spectrum, including tumors with indolent behavior, low-grade malignant potential with locally destructive tumor growth and high local recurrence rates and high-grade malignant potential characterized by risk for disseminated disease and disease-related mortality. Reliable diagnosis to predict behavior may be challenging for a number of reasons. The clinical presentation is often nonspecific. Many of the tumors are rare, and they are only infrequently encountered in routine diagnostic practice. A significant subset of tumors shows bland and innocuous histologic features. They are easily mistaken for benign tumors despite their potential for destructive growth and aggressive disease course. At the other end of the spectrum the tumors may resemble poorly differentiated carcinoma or adenocarcinoma and recognition relies entirely on sampling and careful histological examination. The tumors may be inseparable from cutaneous metastases from visceral primaries by morphology and immunohistochemistry, requiring careful clinical correlation and work-up. Conversely, cutaneous metastases are readily mistaken for cutaneous primary tumors. While the presence of a myoepithelial layer is a helpful feature in excluding metastatic deposits, it does not imply benign behavior of sweat gland tumors in general. The above issues and challenges are exemplified in the discussion of selected sweat gland carcinoma in this manuscript, with a focus on recently described entities and those with novel findings.

Introduction

The diagnosis of sweat gland carcinomas poses a significant challenge for a number of reasons. The tumors show a wide morphologic spectrum, ranging from tumors with bland and innocuous appearances closely mimicking benign skin adnexal tumors to pleomorphic high-grade tumors resembling cutaneous metastases from visceral primaries. The correct diagnosis is largely based on morphologic assessment. Additional tools, such as immunohistochemistry and molecular genetics, play a limited diagnostic role at least at present. The histologic criteria of malignancy are poorly defined for sweat gland neoplasms, and they are often entity

specific. Microcystic adnexal carcinoma, for example, may be impossible to distinguish from benign hair follicle tumors, such as trichoadenoma and desmoplastic trichoe-pithelioma, on partial biopsies [1]. Only the identification of the diffusely infiltrative growth pattern allows reliable separation. Morphologically low-grade spiradenocarcinoma closely resembles a benign spiradenoma on low-power examination [2]. Its diagnosis requires high-power examination with recognition of loss of the dual cell differentiation and the presence of mild cytologic atypia and increased mitotic activity. In contrast, morphologically high-grade spiradenocarcinoma resembles metastatic adenocarcinoma and can only be diagnosed by the presence of a benign spiradenoma precursor [2]. Other primary cutaneous sweat gland tumors show the same morphologic, immunohistochemical, and genetic features as their visceral counterparts and the distinction of a cutaneous primary from a cutaneous metastasis requires close clinical correlation and imaging studies. While the demonstration of a second myoepithelial cell layer using p63 or p40 immunohistochemistry favors a primary cutaneous tumor rather than a metastasis from a visceral primary, its presence does not

✉ Thomas Brenn
thomas.brenn@ucalgary.ca

¹ Department of Pathology and Laboratory Medicine, University of Calgary, Calgary, AB, Canada

² The Arnie Charbonneau Cancer Institute, Cumming School of Medicine, University of Calgary, Calgary, AB, Canada

always imply benign behavior or in situ disease as seen in digital papillary adenocarcinoma [2, 3].

Reliable classification of sweat gland carcinomas is necessary to predict behavior. Malignant sweat gland tumors have traditionally been stratified into those of low-grade malignant potential (Table 1) with locally destructive growth and risk for local recurrence and high-grade malignant tumors (Table 2) with risk for metastasis and disease-related mortality [1, 2]. Certain sweat gland tumors may show significant morphologic variability. In some tumors at least, morphology may be a predictor of outcome (e.g., morphologically low- versus high-grade spiradenocarcinoma), while the disease course of others is entirely independent of morphology (e.g., digital papillary spiradenocarcinoma) [2].

The following section provides an overview and update on selected sweat gland carcinoma to illustrate the aforementioned problem areas. It includes entities that have recently been added to the WHO Classification of Skin Tumors, 4th edition (cribriform carcinoma, endocrine mucin producing carcinoma, secretory carcinoma, and squamoid eccrine carcinoma) and those with novel information (adenoid cystic carcinoma, spiradenocarcinoma, and digital papillary adenocarcinoma).

Cribriform carcinoma

Cribriform carcinoma is a rare but distinctive sweat gland tumor with a predilection for the extremities and an indolent disease course (Table 3).

Clinical features

The tumors present as 1–3 cm nodules with a strong predilection for the upper and lower limbs of middle-aged adults [4–6]. Females are more frequently affected than males.

Histologic features

These nodular but unencapsulated tumors present in mid to deep dermis with occasional involvement of superficial subcutaneous adipose tissue (Fig. 1a). They are composed of basaloid epithelioid to ovoid cells arranged in solid anastomosing nests and groups showing florid duct differentiation, giving rise to the cribriform low-power appearances (Fig. 1b, c). Focal cystic spaces, micropapillary projections, and apocrine differentiation with decapitation secretion may be present (Fig. 1d). The tumor cells contain moderate amounts of cytoplasm and hyperchromatic to vesicular nuclei with small nucleoli. Cytologic atypia is mild, there is no significant nuclear pleomorphism, and mitotic activity is sparse. A second myoepithelial cell layer

Table 1 List of malignant sweat gland tumors with low-grade malignant potential characterized by indolent behavior or locally destructive growth with risk for local recurrence but rare metastatic potential

Sweat gland carcinomas with low-grade malignant potential
Cribriform carcinoma
Secretory carcinoma
Endocrine mucin producing sweat gland carcinoma
Mucinous carcinoma
Microcystic adnexal carcinoma
Squamoid eccrine ductal carcinoma
Adenoid cystic carcinoma
Malignant neoplasms arising from spiradenoma, cylindroma, and spiradenocylindroma; morphologically low-grade

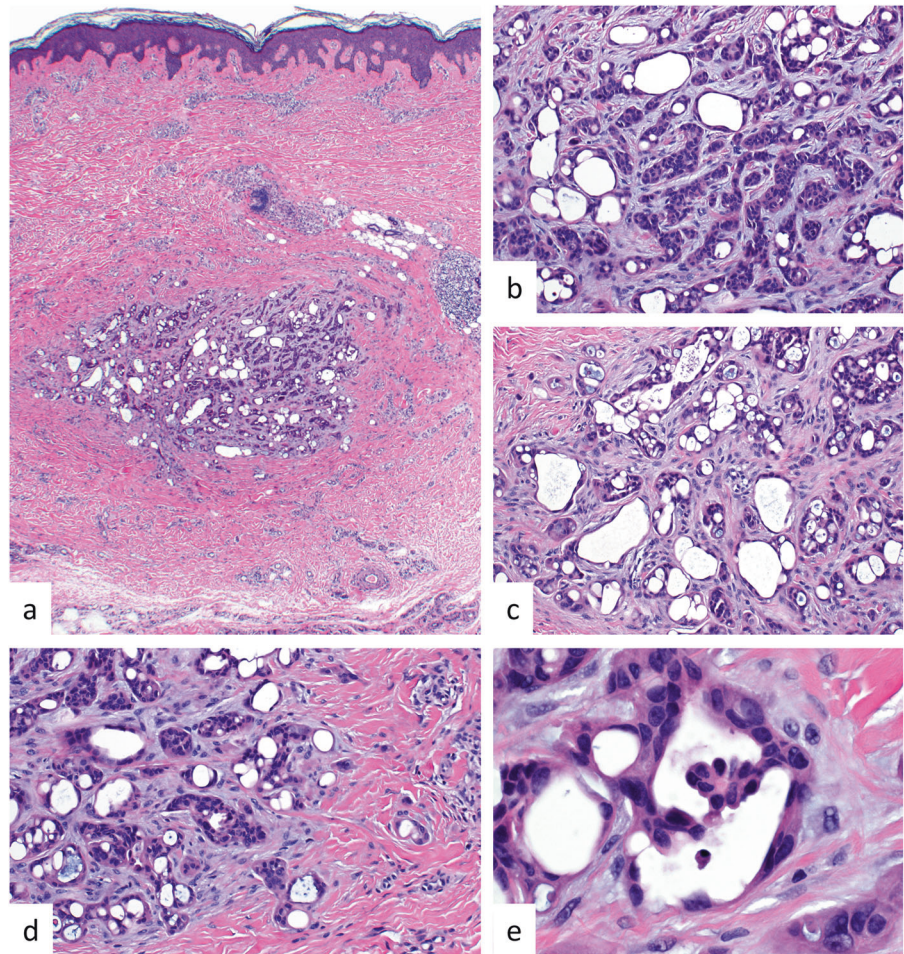
Table 2 List of malignant sweat gland tumors with high-grade malignant potential characterized by metastatic potential and disease-related mortality

Cutaneous sweat gland carcinomas with high-grade malignant potential
Porocarcinoma
Hidradenocarcinoma
Digital papillary adenocarcinoma
Apocrine carcinoma
Syringocystadenocarcinoma papilliferum
Malignant neoplasms arising from spiradenoma, cylindroma, and spiradenocylindroma; morphologically high-grade
Signet-ring cell/histiocytoid carcinoma
Adnexal adenocarcinoma, not otherwise specified

Table 3 Salient clinical, histologic, and immunohistochemical features of cribriform carcinoma

Cribriform carcinoma			
Clinical features	Histologic features	Immunohistochemistry	
Nodules (1–3 cm)	Nodular, circumscribed, unencapsulated	Positive AE1/3	Negative CK20
Limbs	Dermal based, ±superficial subcutis	CK7	GATA3
Middle-aged adults	Anastomosing growth of solid nests	S100	SMA
F > M		CD117	P63
Indolent behavior	Florid lumen formation with cribriform architecture Mild cytologic atypia, scant mitoses Little intervening desmoplastic stroma		

Fig. 1 Cribriform carcinoma. The tumor is characterized by a nodular and relatively circumscribed but unencapsulated architecture within dermis (a). It is composed of anastomosing solid nests of basaloid tumor cells with duct differentiation (b). In areas, florid duct formation gives rise to a cribriform growth pattern (c). The tumor shows and intervening desmoplastic stroma and small tumor nests break off from the main tumor nodule in the periphery (d). A micropapillary growth is a focal finding (e)



is lacking. The edges of the tumor may be irregular, but a truly infiltrative growth pattern is not observed (Fig. 1e). There is scant intratumoral desmoplastic stroma.

By immunohistochemistry, the tumor cells express cytokeratins AE1/3, MNF116, CK5/6, and CK7. They are also positive for EMA, CEA, S100, BerEP4, and CD117. No staining is seen for CK20, SMA, calponin, P63, estrogen receptor, progesterone receptor, androgen receptor, GCDFP15, and GATA3 [5–7].

Prognosis

Cribriform carcinoma shows an indolent disease course following complete excision with no local recurrence, metastasis, or disease-related mortality as yet.

Differential diagnosis

The tumors may be mistaken for adenoid cystic carcinoma, either primary or metastatic to the skin. In contrast to cribriform carcinoma, adenoid cystic carcinoma is

poorly circumscribed and arranged in tumor islands of varying shapes and sizes separated by intervening stroma. Furthermore, it is characterized by mucinous pseudocysts, which are absent in cribriform carcinoma. Tubular adenomas, including papillary eccrine adenoma and apocrine tubular adenoma, show overlapping features with a nodular growth in dermis. The main distinguishing feature is the growth of individual tubules separated by more abundant intervening fibrous stroma and the presence of a myoepithelial cell layer.

Endocrine mucin producing sweat gland carcinoma

Endocrine mucin producing sweat gland carcinoma is a morphologically distinctive neoplasm with neuroendocrine differentiation, resembling solid papillary/endocrine ductal carcinoma of the breast [8]. It shows a narrow anatomic distribution with a strong predilection for the eyelids and cheek and an indolent disease course. It may be a precursor to at least a subset of mucinous carcinoma (Table 4).

Table 4 Salient clinical, histologic, and immunohistochemical features of endocrine mucin producing sweat gland carcinoma

Endocrine mucin producing sweat gland carcinoma			
Clinical features	Histologic features	Immunohistochemistry	
Nodules	Multinodular,	Positive	Negative
Eyelid and cheek	circumscribed, unencapsulated	AE1/3	CK20
Elderly adults	Dermal based,	CK7	S100
F > M	±superficial	GATA3	SMA
Indolent behavior	subcutis	ER, PR	P63
It may be a precursor to at least a subset of mucinous carcinoma	Solid, cribriform, and cystic patterns	MYB	Neuroendocrine marker
	Mucin filled pseudocysts		
	Micropapillary structures		
	Mild cytologic atypia, scant mitoses		

Clinical features

The tumors affect the elderly with a female predominance. They present as slowly enlarging solitary nodular and cystic lesions [9–11]. The lower eyelid is most frequently involved and extrafacial presentation is exceptional.

Histologic features

The tumors show a multinodular and well-circumscribed growth within dermis with occasional additional involvement of superficial subcutaneous adipose tissue (Fig. 2a). They are characterized by a combination of solid, cribriform, cystic, and papillary growth patterns and are composed of basaloid ovoid to epithelioid cells with moderate amounts of cytoplasm containing central nuclei with evenly dispersed chromatin and inconspicuous nucleoli (Fig. 2b, c). Intracellular mucin may be present, but cytologic atypia is scattered and mild and mitoses are sparse (Fig. 2c). The tumor cells show a solid and sheet-like arrangement with additional areas of mucinous pseudocyst formation, giving rise to a cribriform architecture (Fig. 2c). Duct differentiation and cystic elements are further findings and there may be focal papillary growth and apocrine differentiation (Fig. 2d, e). Focal in situ disease with involvement of pre-existing sweat ducts may be present and areas containing extracellular mucin pools raise concern for progression to mucinous carcinoma (Fig. 2f).

By immunohistochemistry, tumor cells express CK7, Cam5.2, EMA, BerEP4, GATA3, WT1, ER, PR, and MYB but they are consistently negative for CK20 (Fig. 3a–c) [9–14]. They also show expression of at least one marker of

neuroendocrine differentiation (Fig. 3d). Focal expression of myoepithelial markers may be seen in the in situ components.

Prognosis

The tumors are indolent. They may recur locally, but metastases or disease-related mortality has not been documented. Complete excision is the recommended treatment.

Differential diagnosis

In view of the presentation on the eyelid sebaceous carcinoma and basal cell carcinoma are important considerations. Sebaceous carcinoma shows a more solid tumor growth with pronounced cytologic atypia and lack of duct/cyst differentiation. The tumors are poorly delineated often with a diffusely infiltrative growth. Recognition of sebaceous differentiation on histology is an important clue to the correct diagnosis. Basal cell carcinoma may show a multinodular tumor growth with mucinous and cribriform areas. The tumors show more significant cytologic atypia, a peripheral palisade, and a surrounding cleft artifact. In contrast to EMPSCG, both basal cell carcinoma and sebaceous carcinoma express P40 and P63 strongly and diffusely and the expression of neuroendocrine markers is distinctly rare. Hidradenoma is another diagnostic pitfall. It shares the multinodular growth and duct and cyst differentiation. The tumor cells show clear cell change or poroid cytologic features and mucinous pseudocysts are not present. Adenoid cystic carcinoma is composed of smaller islands in a diffusely infiltrative growth.

Secretory carcinoma of the skin

Secretory carcinoma rarely affects the skin. It shows similar morphologic, immunohistochemical findings to secretory carcinoma at other sites, particularly the breast and salivary glands, and shares the t(12;15) translocation resulting in the ETV6-NTRAK3 fusion protein (Table 5) [15–18].

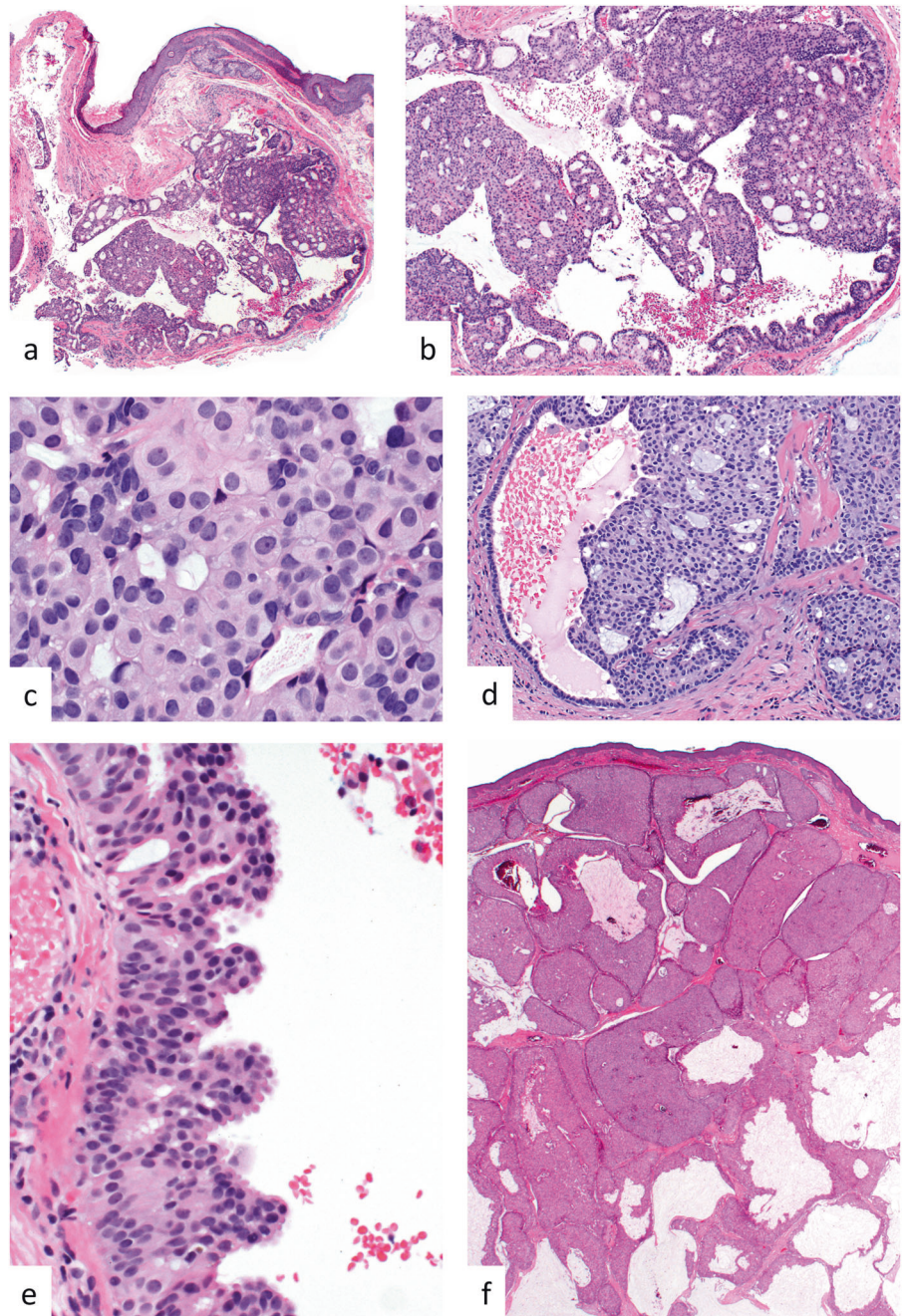
Clinical features

Secretory carcinoma manifesting in the skin is rare. It affects middle aged to elderly patients with a female predilection [15–18]. The tumors are solitary nodules measuring around 1 cm. The axilla is the most commonly affected site.

Histologic features

These nodular tumors are well circumscribed but unencapsulated and present within dermis with possible

Fig. 2 Endocrine mucin producing sweat gland tumor. This multinodular tumor involves mid to deep dermis (a) and is characterized by a combination of solid, cribriform, cystic, and micropapillary growth patterns (b). The tumor is composed of solid sheets of ovoid to epithelioid cells with moderate amounts of cytoplasm and central ovoid to round nuclei with inconspicuous nucleoli. There is intracytoplasmic mucin and mucin filled pseudocysts are present (c). The cribriform appearances are due to the mucin filled pseudocysts. In addition, duct differentiation is present (d). Micropapillary structures showing apocrine differentiation protrude into the cystic spaces (e). A subset of tumors show transition to outright mucinous carcinoma characterized by large pools of extracellular mucin (f)



extension into superficial subcutis (Fig. 4a). They show a solid growth composed of uniform and cytologically bland epithelioid cells with moderate amounts of cytoplasm containing vesicular nuclei and small eosinophilic nucleoli. There is florid microcystic differentiation with numerous intraluminal colloid-like eosinophilic secretions (Fig. 4b). Solid and tubular growth patterns may also be present. Cytologic atypia is limited, the mitotic rate is low, and there is no evidence of necrosis or infiltrative growth.

By immunohistochemistry, tumor cells express AE1/3, Cam5.2, CK7 and S100, mammaglobin, and STAT5a (Fig. 4c, d) [15–17]. In addition, staining may be seen using the anti-pan-NTRK antibody.

Genetic findings

The tumors show a recurrent t(12;15) translocation resulting in an ETV6-NTRK3 fusion gene [16]. A NFIX-PKN1 fusion gene was found in a single tumor [15].

Fig. 3 Endocrine mucin producing sweat gland carcinoma. By immunohistochemistry there is strong and diffuse staining for CK7 (a) and nuclear staining for GATA3 (b) and ER (c). There is expression of at least one neuroendocrine marker. Synaptophysin expression is shown in d

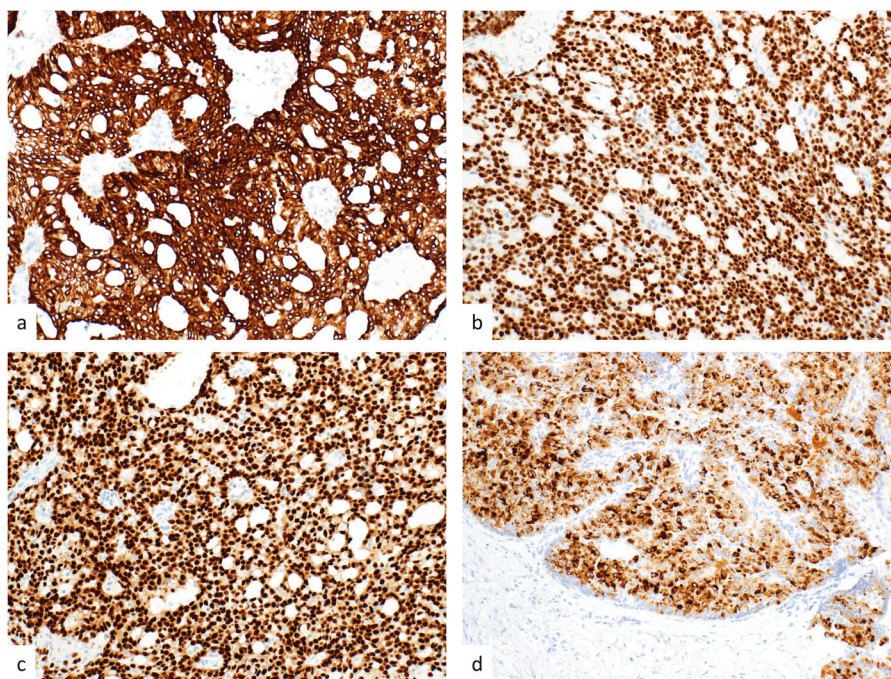


Table 5 Salient clinical, histologic, and immunohistochemical features of secretory carcinoma

Secretory carcinoma			
Clinical features	Histologic features	Immunohistochemistry	
Nodules (1 cm)	Nodular,	Positive	Negative
Axilla	circumscribed,	AE1/3	CK20
Middle-aged to elderly adults	unencapsulated	CK7	
Indolent behavior	Dermal based,	S100	
ETV6-NTRK3 gene fusion	±superficial subcutis	STAT5	
	Solid with microcystic architecture	Mammaglobin	
	Intraluminal colloid secretion	Pan-NTRK	
	Mild cytologic atypia, scant mitoses		

Prognosis

With limited available follow-up the behavior appears to be indolent. Complete excision is advisable.

Differential diagnosis

Secretory carcinoma of the skin shows identical features to tumors of salivary or breast origin and clinical correlation is necessary to exclude a cutaneous metastasis from a visceral primary. Metastasis from a thyroid primary malignancy can be excluded by the absence of TTF-1 staining. Cribriform

carcinoma shows a more cribriform rather than microcystic growth with intervening desmoplastic stroma. Adenoid cystic carcinoma shows a more nested and diffusely infiltrative architecture with the formation of mucinous pseudocysts.

Microcystic adnexal carcinoma

Microcystic adnexal carcinomas are distinctive cutaneous tumors showing follicular and ductal differentiation [19]. They are morphologically bland and are readily mistaken for benign skin adnexal tumors, which may result in destructive tumor growth due to delayed diagnosis and treatment (Table 6).

Clinical features

The tumors present as indurated, slowly enlarging plaques, measuring up to several centimeters. The tumor size is often underestimated clinically. There is a strong predilection for the head, particularly the nasolabial folds and periorbital area, of middle aged to elderly adults [19–23]. The age spectrum is wide but the skin outside the head and neck area is only rarely involved. There is no significant gender predilection.

Histologic features

Microcystic adnexal carcinomas are characterized by follicular and ductal differentiation in varying proportions and

Fig. 4 Secretory carcinoma. These multinodular tumors present in dermis and superficial subcutaneous adipose tissue (**a**). They are composed of uniform epithelioid cells with vesicular nuclei and small nucleoli with florid luminal differentiation giving rise to a microcystic architecture. Also note the intraluminal pink colloid secretions (**b**). The tumor cells express cytokeratin AE1/3 (**c**) and S100 (**d**). Courtesy of Prof. B. Luzar, University of Ljubljana

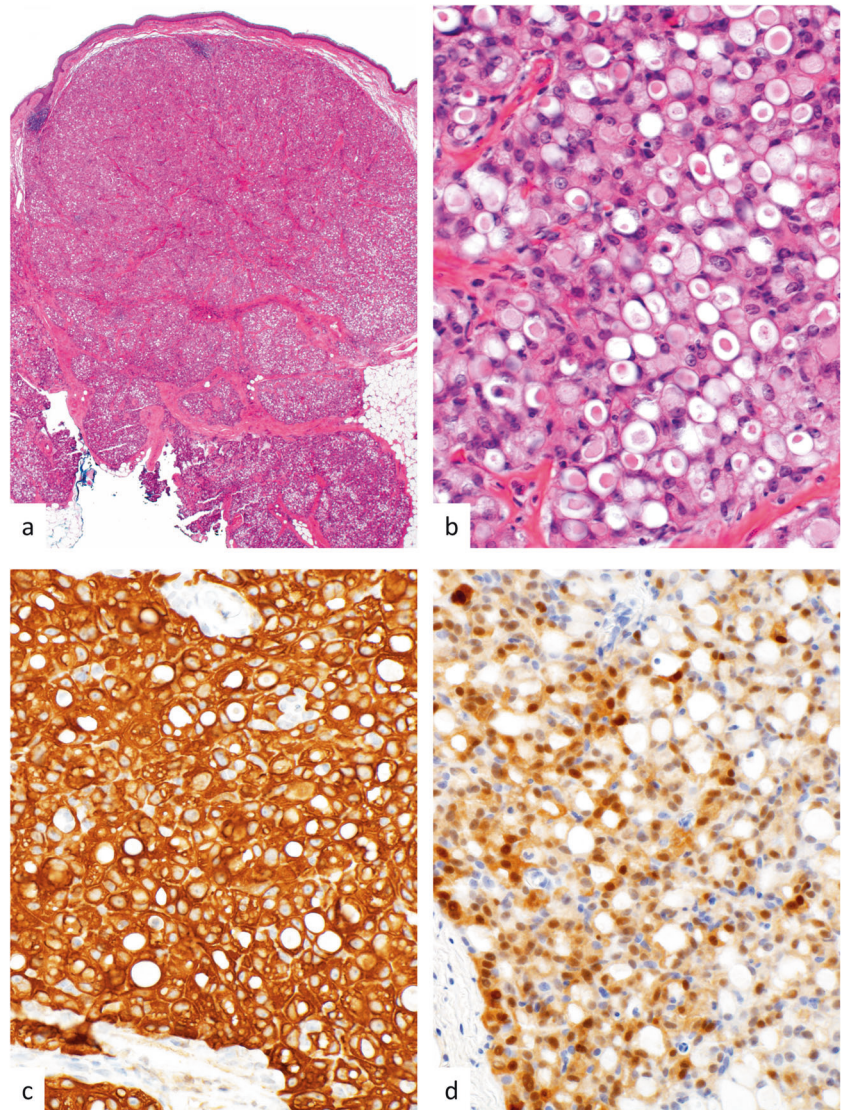


Table 6 Salient clinical and histologic features of microcystic adnexal carcinoma

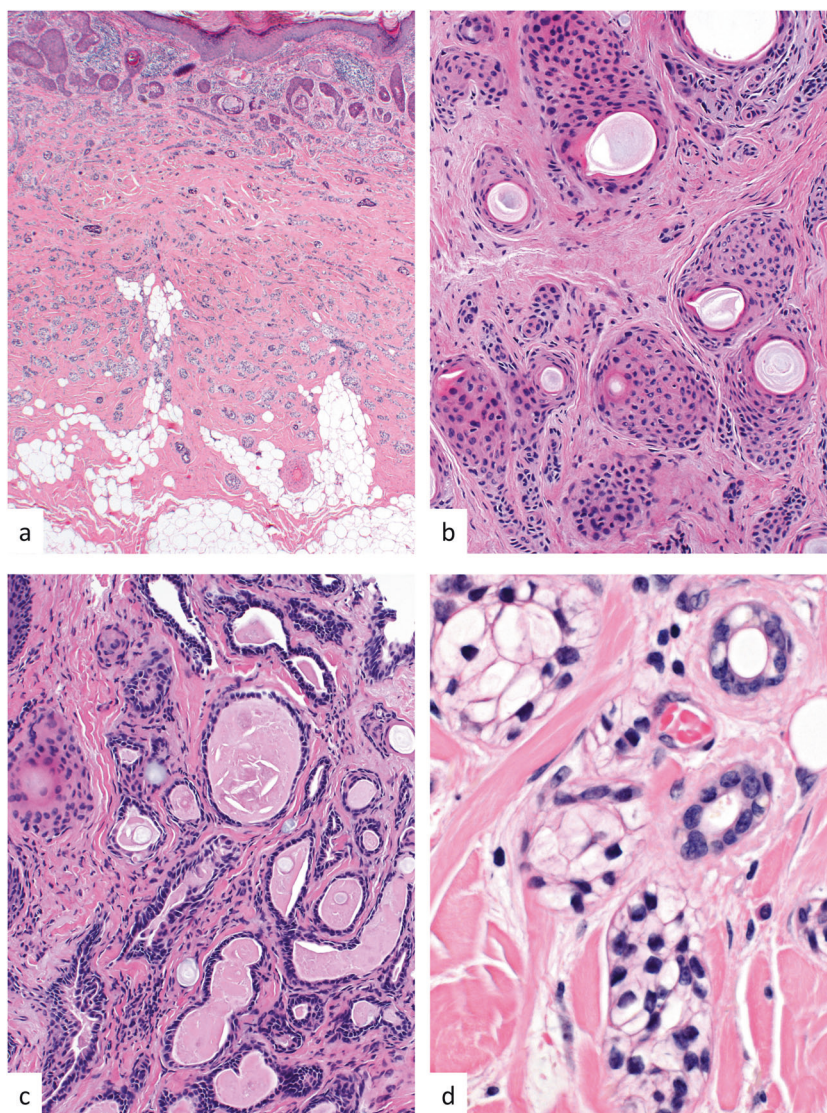
Microcystic adnexal carcinoma	
Clinical features	Histologic features
Indurated plaques	Diffusely infiltrative
Head	Dermal based with invasion of subcutis
Middle-aged to elderly adults	Bland basaloid cords and strands in desmoplastic stroma
Locally destructive growth	Keratocyst formation and calcifications
Risk for local recurrence	Ductal differentiation
	Little cytologic atypia, scant mitoses
	Perineural infiltration

bland cytologic features. These dermal-based tumors show a diffusely infiltrative growth with frequent invasion of underlying subcutaneous adipose tissue, skeletal muscle,

fascia, and even bone (Fig. 5a). They are composed of cords, nests, and strands of basaloid epithelial cells in a desmoplastic stroma (Fig. 5b). Cytologic atypia is mild at most, and mitotic figures are rare. Especially in the superficial aspects, the tumors show keratocyst formation and dystrophic calcifications. A focal connection with the epidermis or a hair follicle is occasionally seen. In addition, the tumor shows areas of duct differentiation characterized by well-formed ducts composed of a single layer of bland appearing ductal cells (Fig. 5c). Other possible findings include clear cell change and a more solid growth pattern (Fig. 5d). Sebaceous differentiation may also be seen. Perineural infiltration is a frequent feature.

By immunohistochemistry, tumor cells express cytokeratin AE1/3, and EMA or CEA staining highlights the luminal differentiation. Expression of BerEP4 is variable and, overall, immunohistochemistry plays no significant role in the diagnosis of these tumors. Diffuse P63 staining

Fig. 5 Microcystic adnexal carcinoma. A diffusely infiltrative growth within dermis with invasion of subcutaneous structures is characteristic (**a**). The tumor is composed of solid strands and nests of bland epithelioid cells. Keratocyst formation is an additional finding (**b**). In other areas, the tumor shows a proliferation of well-formed ducts (**c**). Clear cell change may be encountered in a subset of tumors (**d**)



in this setting supports a primary cutaneous neoplasm and argues against a cutaneous metastasis.

Prognosis

Microcystic adnexal carcinoma carries potential for locally destructive growth and local recurrence if incompletely excised. Metastases and disease-related mortality are exceptional [21]. Early diagnosis and wide local excision or Mohs micrographic surgery are important to prevent against locally aggressive behavior and recurrence [22, 24].

Differential diagnosis

Microcystic adnexal carcinoma is cytologically deceptively bland and may be easily mistaken for desmoplastic trichoepithelioma, trichoadenoma, or syringoma on superficial

shave biopsies where the deeper and more infiltrative aspect of the tumor is not visualized. Syringoma is composed of ductal structures showing short epithelial strands but follicular differentiation with keratocysts is not a feature. Desmoplastic trichoepithelioma and trichoadenoma mimic microcystic adnexal carcinoma very closely. They are well-circumscribed, confined to the superficial and mid dermis, and lack duct differentiation. On a superficial biopsy reliable separation is often not possible and a repeat biopsy or complete excision to include the entire dermis and superficial subcutis is advisable in these instances to exclude the possibility of microcystic adnexal carcinoma. Infiltrative and morpheic basal cell carcinoma resembles certain aspects of microcystic adnexal carcinoma. It invades in a diffusely infiltrative pattern but shows more pronounced cytologic atypia and lacks duct differentiation. Its behavior and treatment are similar to microcystic adnexal carcinoma.

Squamoid eccrine ductal carcinoma

Squamoid eccrine ductal carcinoma is a low-grade, biphasic malignant sweat gland tumor showing areas resembling well- to moderately differentiated squamous cell carcinoma in the superficial aspects and eccrine ductal carcinoma in the deeper reaches of the tumor [25]. The tumors are likely underrecognized and are readily mistaken for squamous cell carcinoma on superficial biopsies. The tumors have also been reported as adenosquamous carcinoma of the skin (Table 7) [26].

Clinical presentation

The tumors present as frequently ulcerated nodules or plaques, measuring around 1 cm, with a predilection for the head and neck area of elderly adults (median age: 80 years) [26, 27]. There is a male predilection.

Histologic features

The tumors are dermal based and show connection with the overlying epidermis, which is frequently ulcerated. They are characterized by a diffusely infiltrative growth, and invasion of subcutaneous tissues is common (Fig. 6a). In the superficial aspect the tumors are composed of atypical keratinocytes arranged in islands and nests of varying sizes, resembling well- to moderately differentiated squamous cell carcinoma (Fig. 6b). A background of squamous cell carcinoma in situ or actinic keratosis may also be present. The deeper aspects of the tumor show a diffusely infiltrative growth of small nests of pleomorphic ductal cells with luminal or duct differentiation (Fig. 6c). Perineural infiltration is a common feature in up to 30% of tumors (Fig. 6d). Lymphovascular invasion is less frequently seen (around 7%).

Immunohistochemical staining for EMA and CEA may help to identify the ductal differentiation, but otherwise immunohistochemistry plays no significant role in the diagnosis of these tumors.

Prognosis

Local recurrence is observed in 25% of patients due to the infiltrative growth of the tumor and the presence of perineural infiltration [27]. Metastases to lymph nodes and disease-related mortality is rare. Wide local excision or Mohs micrographic surgery are the treatments of choice.

Differential diagnosis

The tumors are easily mistaken for squamous cell carcinoma, especially in superficial biopsies in which the

ductal component is not included. Porocarcinoma may show focal squamous differentiation. These tumors arise multifocally from the overlying epidermis in broad bands and are composed of atypical polygonal cells with poroid features. They lack the zonation typical of squamoid eccrine ductal carcinoma. Microcystic adnexal carcinoma is characterized by follicular and ductal differentiation. In contrast to squamoid eccrine ductal carcinoma cytologic atypia is minimal.

Adenoid cystic carcinoma of the skin

Primary cutaneous adenoid cystic carcinoma is a rare tumor showing identical histologic, immunohistochemical, and genetic features to its visceral counterparts, commonly of salivary or lacrimal glands or respiratory tract origin. Clinical correlation is often necessary to exclude the possibility of a cutaneous metastasis from a visceral primary (Table 8).

Clinical features

Cutaneous adenoid cystic carcinoma presents as solitary and slowly growing nodules and plaques, averaging 3 cm in diameter [28, 29]. The tumors affect middle-aged to elderly adults with a median age of 62 years. There is no significant gender predilection. The head and neck, particularly the scalp, are most frequently affected followed by the trunk and the extremities [28, 29].

Histologic features

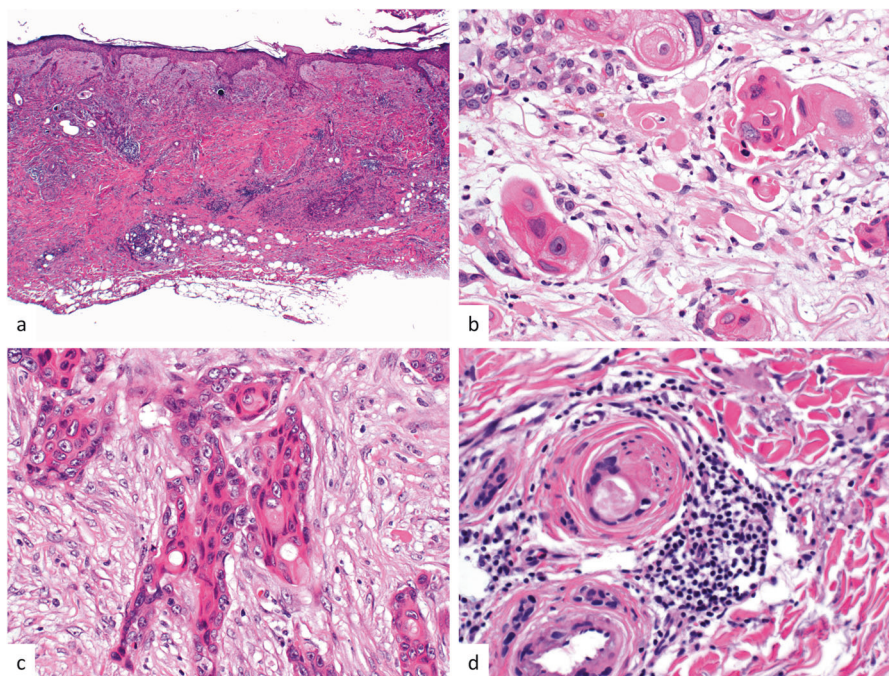
The tumors are characterized by a diffusely infiltrative growth within dermis with frequent invasion of subcutaneous tissues (Fig. 7a). They are arranged in nests and islands of varying shapes and sizes composed of small to medium sized basaloid cells with scanty cytoplasm and hyperchromatic to vesicular nuclei containing variably conspicuous and occasionally multiple nucleoli (Fig. 7b). The tumor cells show a solid or cribriform architecture characterized by mucin filled pseudocysts (Fig. 7c). In addition, the tumor islands may contain hyaline basement membrane protein. True duct differentiation is a focal finding and areas of a tubular growth may be appreciated (Fig. 7d). Nuclear pleomorphism is limited and the mitotic activity is low. Most tumors are grade 1 (Batsakis grading scheme [30]). Perineural infiltration is frequently identified (Fig. 7e).

By immunohistochemistry, tumor cells express cytokeratins. S100, SOX10, and SMA expression is seen in a subset of cells (Fig. 8a). CD117 is diffusely expressed throughout the tumor and there is overexpression of MYB (Fig. 8b, c) [28, 31]. EMA and CEA staining highlights

Table 7 Salient clinical and histologic features of squamoid eccrine ductal carcinoma

Squamoid eccrine ductal carcinoma	
Clinical features	Histologic features
Ulcerated nodules and plaques	Diffusely infiltrative growth in dermis with invasion of subcutis
Head and neck	Multifocal epidermal connection
Elderly adults	Squamous differentiation superficially, resembling squamous cell carcinoma
M > F	Duct differentiation with marked nuclear pleomorphism and mitotic activity in deeper aspect, resembling eccrine ductal carcinoma
Local recurrence	Perineural infiltration
Rare metastatic spread and mortality	Rare lymphovascular invasion

Fig. 6 Squamoid eccrine carcinoma. The tumors are based within dermis and show a diffusely infiltrative growth pattern with invasion of subcutaneous tissues (a). They are further characterized by a biphasic growth with differentiation toward squamous cell carcinoma in the superficial aspects of the tumor (b). The deeper component is characterized by pleomorphic cuboidal cells with duct differentiation in a desmoplastic stroma. The findings are reminiscent of eccrine ductal carcinoma (c). Perineural infiltration is a frequent finding (d)



duct differentiation and collagen IV stains basement membrane material.

Genetic findings

Analogous to adenoid cystic carcinoma of visceral sites, the majority of cutaneous tumors show MYB gene rearrangements including the t(6;9) translocation resulting in the MYB-NFIB gene fusion [31]. Rarely, a fusion gene involving MYBL is detected [32].

Prognosis

Cutaneous adenoid cystic carcinoma shows a high propensity for local recurrence in around 50% [28]. The overall metastatic potential and disease-related mortality is however low, especially when compared with tumors at visceral sites. Tumor metastases are found most frequently in lymph

nodes, lung, and liver. The overall 5-year survival rate is 96% [33]. Tumors arising in the vulva may show more aggressive behavior.

Differential diagnosis

Clinical correlation is necessary to exclude the possibility of a metastasis from a visceral primary adenoid cystic carcinoma. Adenoid basal cell carcinoma lacks true duct differentiation and shows a peripheral palisade and stromal cleft artifact. Cribriform carcinoma lacks the infiltrative growth pattern and shows florid duct differentiation without mucinous pseudocysts. Occasionally, spiradenoma may resemble adenoid cystic carcinoma and shares the overexpression of MYB immunohistochemically. It is characterized by a dual cell population and lacks cytologic atypia, mitotic activity, and perineural infiltration.

Table 8 Salient clinical, histologic, and immunohistochemical features of adenoid cystic carcinoma

Adenoid cystic carcinoma		
Clinical features	Histologic features	Immunohistochemistry
Slowly growing nodules and plaques (3 cm)	Diffusely infiltrative growth in dermis with invasion of subcutis	Positive AE1/3
Head and neck > trunk and extremities	Basaloid nests and islands of varying shapes and sizes	S100 SOX10 SMA
Middle-aged to elderly adults	Mucinous pseudocysts with cribriform architecture	CD117 MYB
Locally destructive growth	Focal duct differentiation and tubular growth	
Local recurrence	Solid, cribriform, and cystic patterns	
Rare metastases and mortality	Mild to moderate cytologic atypia	
	Low mitotic activity	

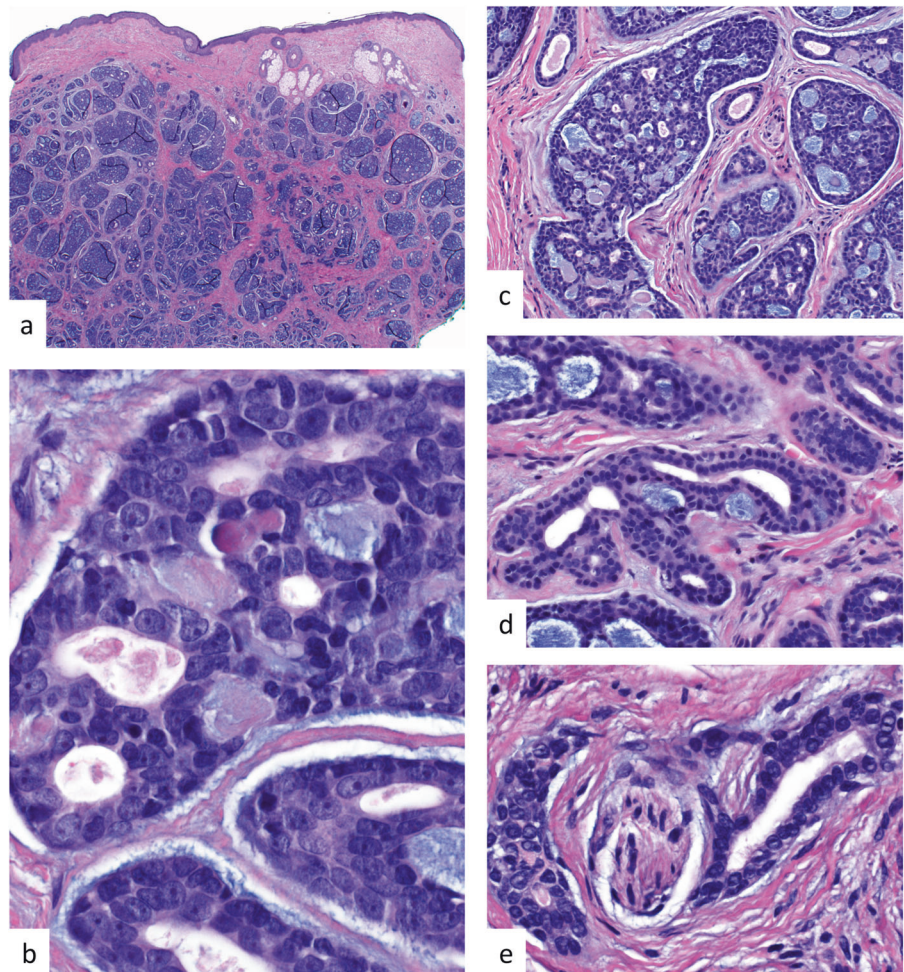
Malignant neoplasms arising from spiradenoma, cylindroma, and spiradenocylindroma

Malignant tumors developing from pre-existing benign spiradenoma, cylindroma, or the spiradenoma-cylindroma hybrid tumors are closely related with similar histological features and behavior [34]. Importantly, identification and recognition of a benign spiradenoma, cylindroma, or spiradenocylindroma precursor is necessary for the diagnosis of these malignant tumors. The majority arises in association with a spiradenoma (Table 9) [34–37].

Clinical features

The tumors are solitary nodules measuring up to multiple centimeters with a median of 2.7 cm [34–37]. There may be a longstanding history with recent growth. The patients are middle aged to elderly adults without gender predominance. A wide range of anatomic locations is affected including the trunk, limbs, and head and neck [34–37]. The vast majority of tumors occur sporadically but rarely they may complicate the autosomal dominant Brooke–Spiegler syndrome.

Fig. 7 Adenoid cystic carcinoma. This basaloid neoplasm is composed of nests and islands diffusely infiltrating dermis (a). The tumor cells contain little cytoplasm with hyperchromatic to vesicular nuclei and prominent and often multiple nucleoli (b). A cribriform growth pattern due to numerous mucin filled pseudocyst is characteristic (c). Additional areas of a tubular growth with true duct differentiation are focally present (d). Perineural infiltration is commonly identified (e)



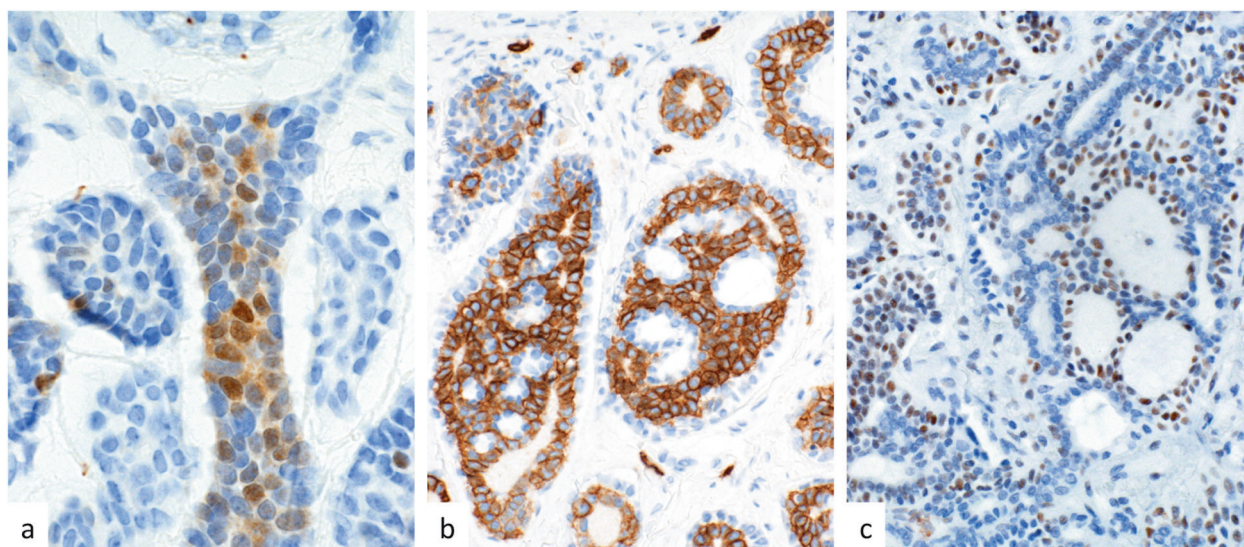


Fig. 8 Adenoid cystic carcinoma. By immunohistochemistry, a subset of the tumor cells expresses S100 (a) and there is strong and diffuse cytoplasmic expression of CD117 (b) and nuclear staining for MYB (c)

Table 9 Salient clinical and histologic features of malignant neoplasms arising from spiradenoma, cylindroma, and spiradenocylindroma

Malignant neoplasms arising from spiradenoma, cylindroma, and spiradenocylindroma		
Clinical features	Histologic features	
	Pre-existing spiradenoma, cylindroma, or spiradenocylindroma	
Nodules (3 cm) Wide anatomic distribution Middle-aged to elderly adults Sporadic but rarely complicates Brooke–Spiegler syndrome Morphologically low grade: indolent behavior Morphologically high grade: risk for disseminated disease and mortality	Low-grade malignant: Loss of dual cell population Uniform basaloid epithelioid cells with mild to moderate atypia Increased mitotic rate	High-grade malignant: Sheets of pleomorphic epithelioid cells ± glandular differentiation Brisk and atypical mitotic activity Tumor necrosis

Histologic features

The malignant component of the tumors shows a wide morphologic spectrum and sampling and recognition of an unequivocal benign spiradenoma, cylindroma or spiradenocylindroma hybrid tumor is necessary for the diagnosis. The tumors are multinodular often with pushing rather than diffusely infiltrative margins. Frequently there is an abrupt transition from the benign precursor to the malignant aspect of the tumor, but occasionally this transition may be more gradual (Fig. 9a). Based on the appearances of the malignant component the tumors are classified morphologically into high grade, low grade, and sarcomatoid. An admixture of different components may be present in a single tumor. Morphologically high-grade tumors are characterized by striking cytologic atypia and nuclear pleomorphism, resembling carcinoma or adenocarcinoma, not otherwise specified (Fig. 9b). The mitotic

activity is brisk including atypical forms and tumor necrosis may be present (Fig. 9c). Lymphovascular invasion and perineural infiltration may also be present. Morphologically low-grade tumors often show a gradual transition from the benign precursor (Fig. 10a). The overall architecture of spiradenoma appears to be retained in the malignant areas at least on low-power examination. Upon closer inspection the low-grade malignant areas are characterized by loss of the dual cell population, characteristic of spiradenoma (Fig. 10b). They are composed of medium sized epithelioid cells with mild to moderate cytologic atypia and increased mitotic activity. Additional features include squamoid differentiation and areas of clear cell change (Fig. 10c). The tumors may be ulcerated and tumor necrosis and perineural infiltration may be observed. Sarcomatoid differentiation is seen most commonly in the form of undifferentiated sarcoma (Fig. 10d). Heterologous chondro-, osteo-, or rhabdosarcomatous elements may also be seen.

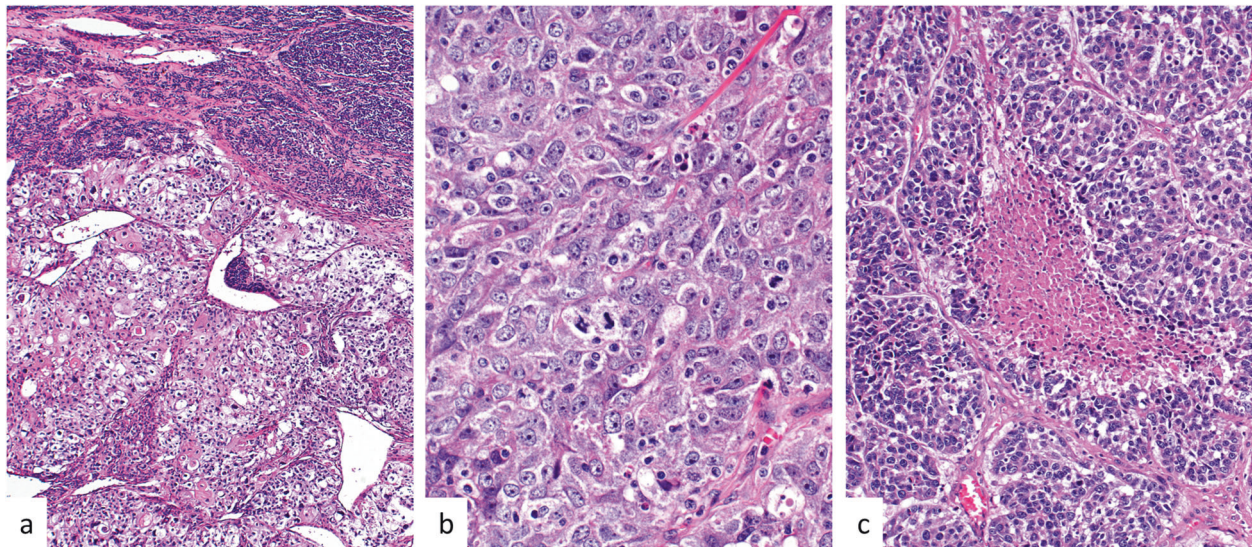


Fig. 9 Spiradenocarcinoma. This morphologically high-grade example shows a sharp demarcation from the benign spiradenoma (seen on top) to the malignant component in the lower aspect (a). It is composed of

sheets of pleomorphic epithelioid cells with brisk and atypical mitotic activity, reminiscent of poorly differentiated carcinoma (b). Tumor necrosis is present (c)

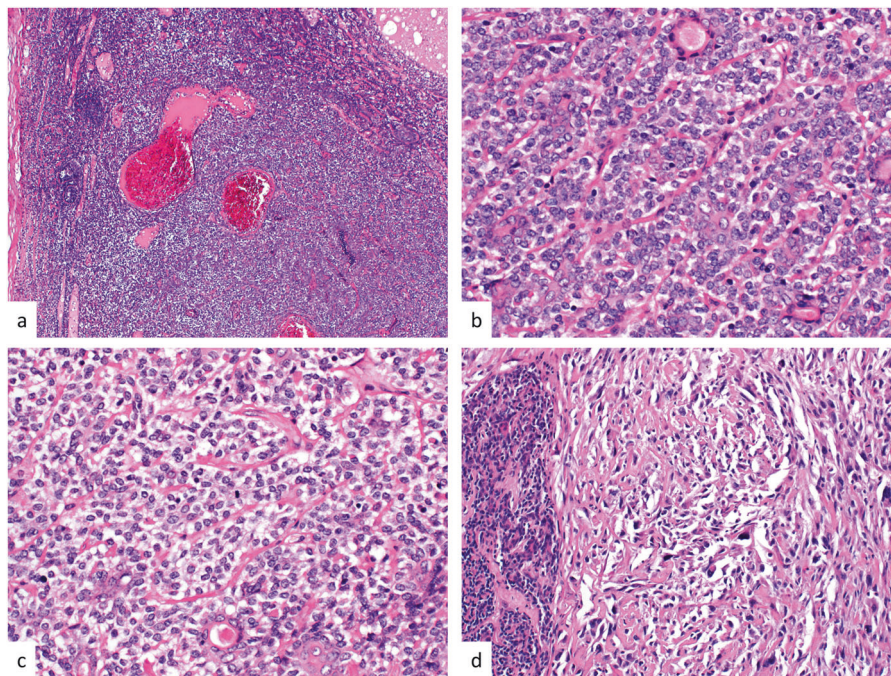


Fig. 10 Spiradenocarcinoma. Morphologically low-grade spiradenocarcinoma shows a pre-existing spiradenoma (on top). The malignant component (lower aspect) retains some of the architectural outlines of its benign precursor and recognition on low-power examination is difficult (a). On higher-power magnification, the malignant component is characterized by a population of epithelioid basaloid

cells showing only mild cytologic atypia (b). Clear cell change and increased mitotic activity may also be encountered (c). Sarcomatoid spiradenocarcinoma is characterized by pleomorphic spindle cells in a collagenous matrix, resembling undifferentiated pleomorphic sarcoma. The correct diagnosis requires sampling and recognition of a benign spiradenoma on the left side of the panel (d)

By immunohistochemistry, spiradenoma, cylindroma, and the hybrid tumors overexpress MYB. Loss of MYB staining is seen in the malignant areas and may be used as an additional marker of malignancy, especially in the

diagnostically challenging low-grade tumors. The mib1-proliferative index is elevated in the malignant areas and there may be P53 overexpression. These findings are however not consistent and lack sensitivity.

Genetic findings

Patients with the Brooke–Spiegler syndrome carry germline mutations in the *CYLD* gene. Similarly, *CYLD* mutations are a consistent finding in sporadic cylindromas [38]. *CYLD* mutations are rare in spiradenomas and their malignant counterparts, which mainly show mutations in the *ALPK1* gene in a mutually exclusive fashion with *CYLD* [38]. *TP53* mutations appear to be associated with malignant transformation.

Prognosis

The behavior of these tumors correlates well with morphology [34, 35, 37]. Morphologically low-grade tumors behave in an indolent fashion with risk for local recurrence in 20% but no metastasis and disease-related mortality [34, 35, 37]. In contrast, the morphologically high-grade tumors show significant potential for distant metastasis and disease-related mortality of up to 50%. Sarcomatous (metaplastic) tumors appear to be at least somewhat less aggressive than their morphologically high-grade counterparts [34].

Differential diagnosis

Morphologically low-grade tumors resemble their benign precursors very closely. Correct diagnosis is possible only on higher-power examination with recognition of the dual cell component, a degree of cytologic atypia, and increased mitotic activity. Absence of *MYB* expression by immunohistochemistry is an additional helpful finding. Morphologically high-grade or sarcomatoid tumors may be mistaken for metastatic carcinoma or adenocarcinoma or undifferentiated sarcoma. Sampling and recognition of a background of a benign spiradenoma, cylindroma, or hybrid tumor are necessary for the correct diagnosis.

Digital papillary adenocarcinoma

These distinctive but diagnostically challenging tumors are confined to the distal extremities of the hands and feet. The tumors show a wide morphologic spectrum, ranging from tumors with bland morphological features to morphologically high-grade examples. Morphologically is however not a predictive of behavior (Table 10) [39–44].

Clinical features

The tumors are present as nodules with a median size of 2 cm. Their anatomic distribution is limited to the hands and feet with a predilection for the distal aspects of the fingers and toes [39–44]. The fingers are more frequently affected than the toes. The age range at presentation is wide and

Table 10 Salient clinical, histologic, and immunohistochemical features of digital papillary adenocarcinoma

Digital papillary adenocarcinoma		
Clinical features	Histologic features	Immunohistochemistry
Nodules (2 cm)	Nodular,	Positive
Hands and feet	circumscribed,	AE1/3
Wide age	unencapsulated	S100
distribution	Rarely infiltrative	Myoepithelial cell layer:
M > F	Dermal based,	SMA
Potential for	±superficial subcutis	Calponin
disseminated	Solid and cystic with	P63
disease and	tubular and papillary	P40
mortality	differentiation	
	Morphologically low-	
	to high-grade without	
	impact on behavior	
	Preserved second	
	myoepithelial	
	cell layer	

includes children, adolescents, and adults with a peak for middle-aged adults [39–44]. There is a strong male predilection.

Histologic features

The tumors are multinodular with a solid and cystic growth in dermis and/or superficial subcutis (Fig. 11a). The tumors are frequently well-circumscribed and papillary differentiation is a typical feature (Fig. 11b). An infiltrative growth pattern is rare. The morphologic spectrum is wide, ranging from bland, innocuous appearances to those with high-grade histologic features, including marked nuclear pleomorphism, brisk and atypical mitotic activity, and tumor necrosis. The solid areas of the tumor are composed of sheets of epithelioid cells with varying degrees of cytologic atypia and nuclear pleomorphism, ranging from mild to severe. Mitotic activity is variable and atypical mitoses as well as tumor necrosis may be found (Fig. 11c, d). Duct differentiation and a tubular growth are typically observed (Fig. 11e). Additional findings are focal clear cell change, spindle cell differentiation, and squamoid differentiation. The cystic spaces are lined by a layer of ductal cell population showing similar cytologic features to the solid areas. In addition, there is an outer, second myoepithelial cell layer (Fig. 11f). The papillary structures include both micro- and micropapillary with fibrovascular cores. They arise from the cyst lining and protrude into the cystic spaces. Focal apocrine differentiation may also be present.

By immunohistochemistry, the tumor cells express cytokeratins strongly and diffusely (Fig. 12a). There is multifocal expression of EMA, which also highlights ductal lumina. A subset of the tumor cells expresses S100 (Fig. 12b) and the outer myoepithelial cell layer is

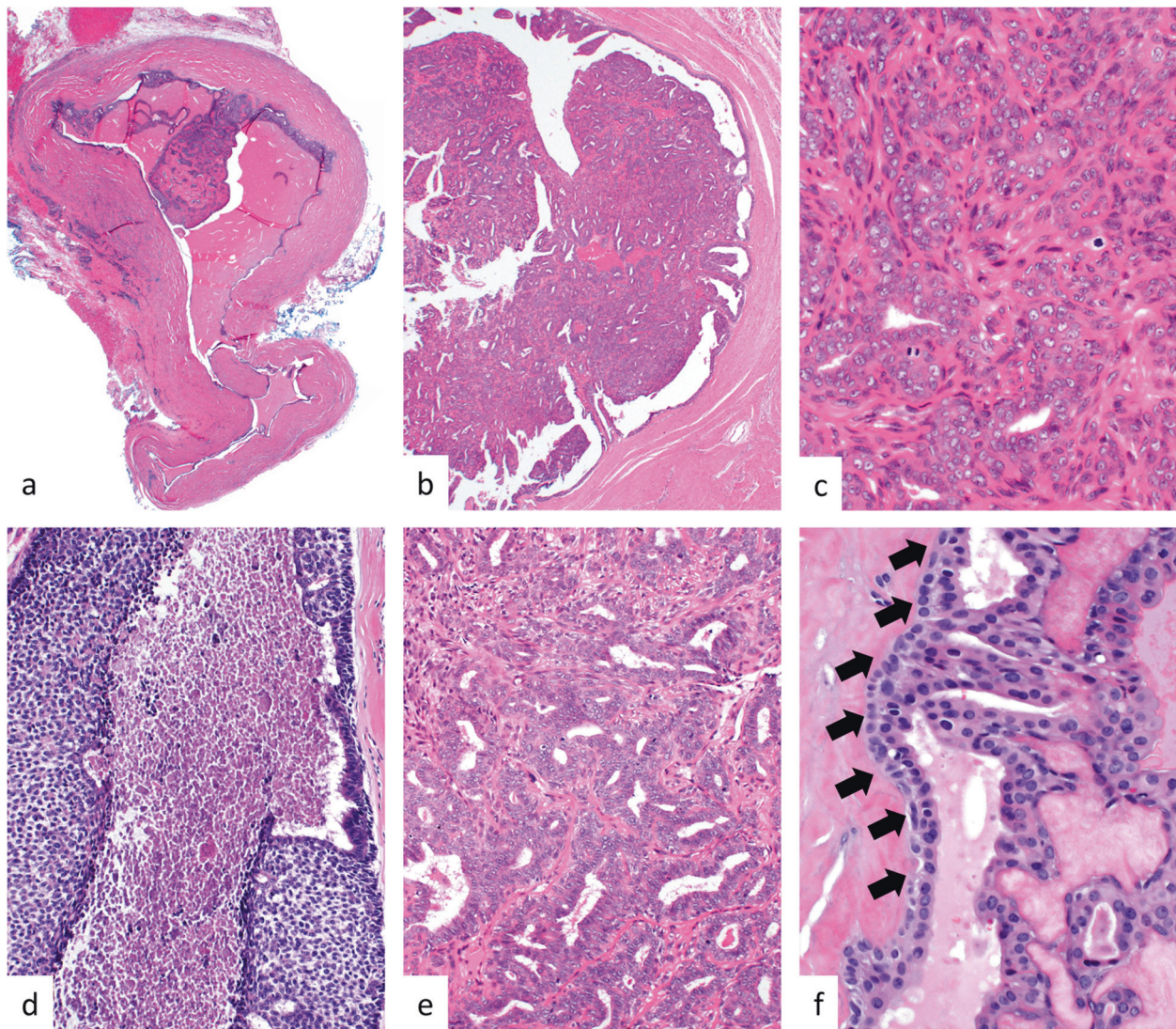


Fig. 11 Digital papillary adenocarcinoma. This well-circumscribed subcutaneous neoplasm shows a predominantly cystic growth with focal papillary and solid areas (a). Micro- and micropapillary structures characterize this nodular tumor (b). Duct differentiation is a characteristic feature, in this example showing higher grade cytologic

atypia and brisk mitotic activity (c). Solid areas and tumor necrosis may be present (d) and a tubular architecture is frequently encountered (e). Cytologic atypia may be minimal but an outer second myoepithelial cell layer (arrows) is invariably present (f)

characterized by expression of SMA, calponin, P63, and P40 (Fig. 12c, d).

Genetic findings

Limited data are available, but no recurrent genetic abnormalities have been identified as yet [45]. Transcriptome analysis has shown overexpression of FGFR2 [46].

Prognosis

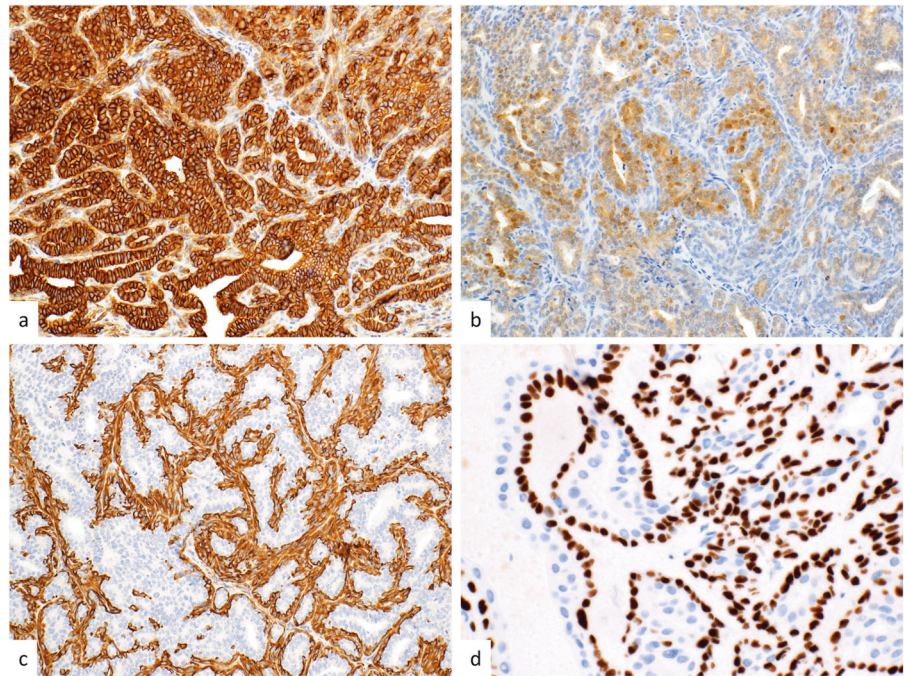
Digital papillary adenocarcinoma shows significant potential for aggressive behavior. Local recurrence rates are high,

especially if inadequately excised, and the tumors have an around 15% metastatic risk to lymph nodes and lung with possibility for disease-related mortality [39–44, 47]. The disease course may be protracted, and metastases and mortality may occur years to decades after the initial presentation. Wide local excision or amputation are the treatment of choice and long-term follow-up is necessary. Importantly the behavior is independent of the morphologic features [39–44].

Differential diagnosis

Morphologically bland appearing tumors are readily mistaken for apocrine cystadenoma or hidradenoma.

Fig. 12 Digital papillary adenocarcinoma. By immunohistochemistry, the tumor cells express cytokeratin AE1/3 strongly and diffusely (a). There is co-expression of S100 in a subset of tumor cells (b). The second myoepithelial cell layer can be highlighted with smooth muscle actin (c) and P40 (d) staining



Apocrine cystadenoma typically affects the face and is exceedingly rare on the digits. The diagnosis should be rendered with care and only after careful examination. Any papillary change or cytologic atypia should be a warning sign that the tumors may represent a digital papillary adenocarcinoma. Hidradenoma lacks the papillary growth and cytologic atypia. Separation from hidradenocarcinoma is largely academic and the behavior is similar. The morphologic high-grade end of the spectrum of digital papillary adenocarcinoma may be mistaken for a cutaneous metastasis of a visceral primary. The presence of a myoepithelial component is a helpful distinguishing feature.

Conclusion

Over the past decade our understanding of the biology of malignant sweat gland tumors has significantly improved, and many of the entities have been defined more precisely. Despite the wide morphologic spectrum and rarity of the tumors outlined above, reliable diagnosis and prediction of behavior is possible with awareness of the subtle morphologic and immunohistochemical distinguishing features and associated diagnostic pitfalls.

Compliance with ethical standards

Conflict of interest The author declare that he has no conflict of interest.

Publisher's note Springer Nature remains neutral with regard to jurisdictional claims in published maps and institutional affiliations.

References

1. van der Horst MPJ, Brenn T. Update on malignant sweat gland tumors. *Surg Pathol Clin.* 2017;10:383–97.
2. Flux K, Brenn T. Cutaneous sweat gland carcinomas with basoid differentiation: an update with emphasis on differential diagnoses. *Clin Lab Med.* 2017;37:587–601.
3. Lee JJ, Mochel MC, Piris A, et al. p40 exhibits better specificity than p63 in distinguishing primary skin adnexal carcinomas from cutaneous metastases. *Hum Pathol.* 2014;45:1078–83.
4. Adamski H, Le Lan J, Chevrier S, et al. Primary cutaneous cribriform carcinoma: a rare apocrine tumour. *J Cutan Pathol.* 2005;32:577–80.
5. Arps DP, Chan MP, Patel RM, Andea AA. Primary cutaneous cribriform carcinoma: report of six cases with clinicopathologic data and immunohistochemical profile. *J Cutan Pathol.* 2015;42:379–87.
6. Rutten A, Kutzner H, Mentzel T, et al. Primary cutaneous cribriform apocrine carcinoma: a clinicopathologic and immunohistochemical study of 26 cases of an under-recognized cutaneous adnexal neoplasm. *J Am Acad Dermatol.* 2009;61:644–51.
7. Llamas-Velasco M, Perez-Gonzalez YC, Dauden E, Rutten A. GATA3 staining in primary cutaneous apocrine cribriform carcinoma: usefulness to differentiate it from breast cancer metastasis. *J Cutan Pathol.* 2018;45:348–51.
8. Flieder A, Koerner FC, Pilch BZ, Maluf HM. Endocrine mucin-producing sweat gland carcinoma: a cutaneous neoplasm analogous to solid papillary carcinoma of breast. *Am J Surg Pathol.* 1997;21:1501–6.
9. Zembowicz A, Garcia CF, Tannous ZS, et al. Endocrine mucin-producing sweat gland carcinoma: twelve new cases suggest that it is a precursor of some invasive mucinous carcinomas. *Am J Surg Pathol.* 2005;29:1330–9.

10. Shon W, Salomao DR. WT1 expression in endocrine mucin-producing sweat gland carcinoma: a study of 13 cases. *Int J Dermatol.* 2014;53:1228–34.
11. Qin H, Moore RF, Ho CY, et al. Endocrine mucin-producing sweat gland carcinoma: a study of 11 cases with molecular analysis. *J Cutan Pathol.* 2018. [Epub ahead of print].
12. Abdulkader M, Kuhar M, Hattab E, Linos K. GATA3 positivity in endocrine mucin-producing sweat gland carcinoma and invasive mucinous carcinoma of the eyelid: report of 2 cases. *Am J Dermatopathol.* 2016;38:789–91.
13. Chou YH, Chang YC, Huang YL, Wu CT. Endocrine mucin-producing sweat gland carcinoma with GATA3 expression: report of two cases. *Pathology.* 2017;49:805–8.
14. Held L, Ruetten A, Kutzner H, et al. Endocrine mucin-producing sweat gland carcinoma: clinicopathologic, immunohistochemical, and molecular analysis of 11 cases with emphasis on MYB immunoexpression. *J Cutan Pathol.* 2018. [Epub ahead of print].
15. Kastnerova L, Luzar B, Goto K, et al. Secretory carcinoma of the skin: report of 6 cases, including a case with a novel NF1X-PKNI translocation. *Am J Surg Pathol.* 2019;43:1092–8.
16. Bishop JA, Taube JM, Su A, et al. Secretory carcinoma of the skin harboring ETV6 gene fusions: a cutaneous analogue to secretory carcinomas of the breast and salivary glands. *Am J Surg Pathol.* 2017;41:62–6.
17. Kazakov DV, Hantschke M, Vanecek T, Kacerovska D, Michal M. Mammary-type secretory carcinoma of the skin. *Am J Surg Pathol.* 2010;34:1226–7. author reply 8.
18. Brandt SM, Swistel AJ, Rosen PP. Secretory carcinoma in the axilla: probable origin from axillary skin appendage glands in a young girl. *Am J Surg Pathol.* 2009;33:950–3.
19. Goldstein DJ, Barr RJ, Santa Cruz DJ. Microcystic adnexal carcinoma: a distinct clinicopathologic entity. *Cancer.* 1982;50:566–72.
20. King BJ, Tolkachjov SN, Winchester DS, et al. Demographics and outcomes of microcystic adnexal carcinoma. *J Am Acad Dermatol.* 2018;79:756–8.
21. Yu JB, Blitzblau RC, Patel SC, Decker RH, Wilson LD. Surveillance, epidemiology, and end results (SEER) database analysis of microcystic adnexal carcinoma (sclerosing sweat duct carcinoma) of the skin. *Am J Clin Oncol.* 2010;33:125–7.
22. Chiller K, Passaro D, Scheuller M, et al. Microcystic adnexal carcinoma: forty-eight cases, their treatment, and their outcome. *Arch Dermatol.* 2000;136:1355–9.
23. LeBoit PE, Sexton M. Microcystic adnexal carcinoma of the skin. A reappraisal of the differentiation and differential diagnosis of an underrecognized neoplasm. *J Am Acad Dermatol.* 1993;29:609–18.
24. Friedman PM, Friedman RH, Jiang SB, et al. Microcystic adnexal carcinoma: collaborative series review and update. *J Am Acad Dermatol.* 1999;41:225–31.
25. Wong TY, Suster S, Mihm MC. Squamoid eccrine ductal carcinoma. *Histopathology.* 1997;30:288–93.
26. Fu JM, McCalmont T, Yu SS. Adenosquamous carcinoma of the skin: a case series. *Arch Dermatol.* 2009;145:1152–8.
27. van der Horst MP, Garcia-Herrera A, Markiewicz D, et al. Squamoid eccrine ductal carcinoma: a clinicopathologic study of 30 cases. *Am J Surg Pathol.* 2016;40:755–60.
28. Ramakrishnan R, Chaudhry IH, Ramdial P, et al. Primary cutaneous adenoid cystic carcinoma: a clinicopathologic and immunohistochemical study of 27 cases. *Am J Surg Pathol.* 2013;37:1603–11.
29. Seab JA, Graham JH. Primary cutaneous adenoid cystic carcinoma. *J Am Acad Dermatol.* 1987;17:113–8.
30. Batsakis JG, Luna MA, el-Naggar A. Histopathologic grading of salivary gland neoplasms: III. Adenoid cystic carcinomas. *Ann Otol Rhinol Laryngol.* 1990;99:1007–9.
31. North JP, McCalmont TH, Fehr A, et al. Detection of MYB alterations and other immunohistochemical markers in primary cutaneous adenoid cystic carcinoma. *Am J Surg Pathol.* 2015;39:1347–56.
32. Kyrpychova L, Vanecek T, Grossmann P, et al. Small subset of adenoid cystic carcinoma of the skin is associated with alterations of the MYBL1 gene similar to their extracutaneous counterparts. *Am J Dermatopathol.* 2018;40:721–6.
33. Dores GM, Huycke MM, Devesa SS, Garcia CA. Primary cutaneous adenoid cystic carcinoma in the United States: incidence, survival, and associated cancers, 1976 to 2005. *J Am Acad Dermatol.* 2010;63:71–8.
34. Kazakov DV, Zelger B, Rutten A, et al. Morphologic diversity of malignant neoplasms arising in preexisting spiradenoma, cylindroma, and spiradenocylindroma based on the study of 24 cases, sporadic or occurring in the setting of Brooke-Spiegler syndrome. *Am J Surg Pathol.* 2009;33:705–19.
35. Granter SR, Seeger K, Calonje E, Busam K, McKee PH. Malignant eccrine spiradenoma (spiradenocarcinoma): a clinicopathologic study of 12 cases. *Am J Dermatopathol.* 2000;22:97–103.
36. Dai B, Kong YY, Cai X, Shen XX, Kong JC. Spiradenocarcinoma, cylindrocarcinoma and spiradenocylindrocarcinoma: a clinicopathological study of nine cases. *Histopathology.* 2014; 65:658–66.
37. van der Horst MP, Marusic Z, Hornick JL, Luzar B, Brenn T. Morphologically low-grade spiradenocarcinoma: a clinicopathologic study of 19 cases with emphasis on outcome and MYB expression. *Mod Pathol.* 2015;28:944–53.
38. Rashid M, van der Horst M, Mentzel T, et al. ALPK1 hotspot mutation as a driver of human spiradenoma and spiradenocarcinoma. *Nat Commun.* 2019;10:2213.
39. Kao GF, Helwig EB, Graham JH. Aggressive digital papillary adenoma and adenocarcinoma. A clinicopathological study of 57 patients, with histochemical, immunopathological, and ultrastructural observations. *J Cutan Pathol.* 1987;14:129–46.
40. Duke WH, Sherrod TT, Lupton GP. Aggressive digital papillary adenocarcinoma (aggressive digital papillary adenoma and adenocarcinoma revisited). *Am J Surg Pathol.* 2000; 24:775–84.
41. Suchak R, Wang WL, Prieto VG, et al. Cutaneous digital papillary adenocarcinoma: a clinicopathologic study of 31 cases of a rare neoplasm with new observations. *Am J Surg Pathol.* 2012;36:1883–91.
42. Scolyer RA, Karim RZ, Thompson JF, et al. Digital papillary adenocarcinoma: a tumour that should be considered in the differential diagnosis of neoplasms involving the digits. *Pathology.* 2013;45:55–61.
43. Molina-Ruiz AM, Llamas-Velasco M, Rutten A, Cerroni L, Requena L. “Apocrine hidrocystoma and cystadenoma”-like tumor of the digits or toes: a potential diagnostic pitfall of digital papillary adenocarcinoma. *Am J Surg Pathol.* 2016;40:410–8.
44. Weingartner N, Gressel A, Battistella M, Cribier B. Aggressive digital papillary adenocarcinoma: a clinicopathological study of 19 cases. *J Am Acad Dermatol.* 2017;77:e1.
45. Bell D, Aung P, Prieto VG, Ivan D. Next-generation sequencing reveals rare genomic alterations in aggressive digital papillary adenocarcinoma. *Ann Diagn Pathol.* 2015;19:381–4.
46. Surowy HM, Giesen AK, Otte J, et al. Gene expression profiling in aggressive digital papillary adenocarcinoma sheds light on the architecture of a rare sweat gland carcinoma. *Br J Dermatol.* 2019;180:1150–60.
47. Rismiller K, Knackstedt TJ. Aggressive digital papillary adenocarcinoma: population-based analysis of incidence, demographics, treatment, and outcomes. *Dermatol Surg.* 2018;44:911–7.